



Research paper

The New Family of Adaptive Filter Algorithms for Block-Sparse System Identification

E. Heydari¹, M. Shams Esfand Abadi^{1,*}, S. M. Khademiyan²

¹Faculty of Electrical Engineering, Shahid Rajaei Teacher Training University, Tehran, Iran.

²Department of Applied Mathematics, Shahid Rajaei Teacher Training University, Tehran, Iran.

Article Info

Article History:

Received 22 July 2023
Reviewed 02 August 2023
Revised 16 September 2023
Accepted 11 October 2023

Keywords:

Block sparse
 $L_{2,0}$ -norm
IMSAF
Selective regressors
Dynamic selection

*Corresponding Author's Email
Address: mshams@sru.ac.ir

Abstract

Background and Objectives: In order to improve the performance of normalized subband adaptive filter algorithm (NSAF) for identifying the block-sparse (BS) systems, this paper introduces the novel adaptive algorithm which is called BSNSAF. In the following, an improved multiband structured subband adaptive filter (IMSAF) algorithms for BS system identification is also proposed. The BS-IMSAF has faster convergence speed than BS-NSAF. Since the computational complexity of BS-IMSAF is high, the selective regressor (SR) and dynamic selection (DS) approaches are utilized and BS-SR-IMSAF and BS-DS-IMSAF are introduced. Furthermore, the theoretical steady-state performance analysis of the presented algorithms is studied.

Methods: All algorithms are established based on the $L_{2,0}$ -norm constraint to the proposed cost function and the method of Lagrange multipliers is used to optimize the cost function.

Results: The good performance of the proposed algorithms is demonstrated through several simulation results in the system identification setup. The algorithms are justified and compared in various scenarios and optimum values of the parameters are obtained. Also, the computational complexity of different algorithms is studied. In addition, the theoretical steady state values of mean square error (MSE) values are compared with simulation values.

Conclusion: The BS-NSAF algorithm has better performance than NSAF for BS system identification. The BSIMSAF algorithm has better convergence speed than BS-NSAF. To reduce the computational complexity, the BS-SR-IMSAF and BS-DSR-IMSAF algorithms are developed. These algorithms have close performance to BS-IMSAF.

This work is distributed under the CC BY license (<http://creativecommons.org/licenses/by/4.0/>)



Introduction

The least mean squares (LMS) and the normalized LMS (NLMS) algorithms are widely used in many adaptive filter applications [1]-[4]. These algorithms are simple, stable and easy to implement [5]. However, the convergence speed of LMS and NLMS algorithms is significantly deteriorated in case of colored input signals. To improve the convergence speed of these algorithms, different algorithms such as affine projection (AP) and normalized

subband adaptive filter (NSAF) algorithms were introduced [6], [7]. Also, the methods of APA and NSAF were combined and improved multiband structured SAF (IMSAF) was proposed in [8], [9]. Since the computational complexity of APA and IMSAF is high, various approaches such as selective regressor (SR) and dynamic selection regressor (DSR) were applied in APA [10], [11] and IMSAF [12]-[14] as well as wavelet transform domain LMS (WTDLMS) [15].

In some applications, the unknown system to be

identified is sparse or block-sparse (BS). It means that the unknown system consists of many zero or near-zero coefficients and a small number of large ones. The typical sparse systems are digital TV transmission channels and echo paths [16]. Also, in satellite-linked or in-door MIMO communications, the impulse response is block sparse. The classical adaptive filter algorithms such as NLMS, APA, NSAF, and IMSAF suffer from poor performance when the impulse response of the unknown system is sparse or block sparse [17].

To solve this problem, the L_0 -norm constraint are utilized in the cost function of various adaptive filter algorithms. In [18], the L_0 -LMS was presented which shows better performance than LMS and NLMS in sparse system identifications. Also, two types of L_0 -APA and L_0 -NSAF algorithms were proposed in [6], [7]. The other researches on sparse systems can be found in [20], [23], [24], and [25]. Furthermore, in our recent research, we introduced the L_0 -IMSAF algorithm [26]. As we mentioned, there is a special sparse system which is called block-sparse (BS). The impulse response of block-sparse system consists of one or more clusters, wherein a cluster is a gathering of nonzero coefficients. In this situation, the sparse adaptive algorithm such as L_0 -LMS doesn't work well. Therefore, the BS-LMS was introduced [27]. The BS-LMS has much better convergence speed than L_0 -LMS in BS system identification. In BS-LMS, a penalty of BS, which is mixed $L_{2,0}$ -norm of adaptive filter coefficients with equal group partition sizes, is inserted to the cost function of LMS. This approach was successfully extended to proportionate NLMS in [28].

In the present study, the BS-NSAF algorithm is firstly introduced. The BS-NSAF has faster convergence speed than L_0 -NSAF in block-sparse systems. Then, to improve the performance of BS-NSAF, the BS-IMSAF is presented. Both algorithms are established based on the $L_{2,0}$ -norm constraint to the proposed cost function. In the following, we introduce two new algorithms to reduce the computational complexity of BS-IMSAF. The SR and DSR approaches are extended to BS-IMSAF and BS-SR-IMSAF and BS-DSR-IMSAF are established. In BS-SR-IMSAF, a subset of the input regressors at each subband are optimally selected during the adaptation. The subsets with dynamic number of members from the input regressors (DSR) at each subband are chosen for every iteration in BS-DSR-IMSAF. Furthermore, the theoretical steady-state performance analysis of the proposed algorithms is also studied. Table 1 reviews the classical, sparse, and BS adaptive filter algorithms. The proposed algorithms have been indicated in Table 1. Also, Table 2 compares the cost functions of L_0 -LMS, BS-LMS, L_0 -NSAF, IMSAF, and proposed BS-NSAF and BS-IMSAF algorithms. In the following, the notations in this table will be illustrated.

Table 1: The L_0 -norm constraint adaptive filter algorithms

Algorithm	Algorithm based on Block Sparse
LMS	L_0 -LMS [18], BS-LMS [27]
NSAF	ZN-NSAF [19], BS-NSAF *
IMSAF	BS-IMSAF *
SR-IMSAF [12]	BS-SR -IMSAF *
DSR-IMSAF [12]	BS-DSR-IMSAF *

* Proposed in this paper.

Table 2: Review of cost functions

Adaptive filter algorithm	Cost function
L_0 -LMS [18]	$J(k) = e(k) ^2 + \delta \ \mathbf{h}(k) \ _0$
BS-LMS [27]	$J(k) = e(k) ^2 + \delta \ \mathbf{h}(k) \ _{2,0}$
ZN-NSAF-I [19]	$J(n) = \ \mathbf{h}(n+1) - \mathbf{h}(n) \ ^2 + \sum_{i=1}^N \lambda_i [d_{i,D}(n) - \mathbf{u}_i^T(n) \mathbf{h}(n+1)]$
ZN-NSAF-II [19]	$J(n) = \frac{1}{2} \sum_{i=1}^N \left(\frac{e_{i,D}(n)}{\ \mathbf{u}_i(n) \ _2} \right)^2 + \frac{1}{2} \delta \ \mathbf{h}(n) \ _0$
IMSAF [12], [13]	$J(n) = \ \mathbf{h}(n+1) - \mathbf{h}(n) \ ^2 + \sum_{i=1}^N \Lambda_i [d_{i,D}(n) - \mathbf{u}_i^T(n) \mathbf{h}(n+1)]$
IMSAF	$J(n) = \frac{1}{2} \sum_{i=1}^N \mathbf{e}_{i,D}^T(n) [\mathbf{U}_i^T(n) \mathbf{U}_i(n)]^{-1} \mathbf{e}_{i,D}(n)$
BS-NSAF *	$J(n) = \frac{1}{2} \sum_{i=1}^N \frac{ e_{i,D}(n) ^2}{\ \mathbf{u}_i(n) \ ^2} + \delta \ \mathbf{h}(n) \ _{2,0}$
BS-IMSAF *	$J(n) = \frac{1}{2} \sum_{i=1}^N \mathbf{e}_{i,D}^T(n) [\mathbf{U}_i^T(n) \mathbf{U}_i(n)]^{-1} \mathbf{e}_{i,D}(n) + \delta \ \mathbf{h}(n) \ _{2,0}$

* Proposed in this paper.

What we propose in this paper can be summarized as follows:

- Establishment of the BS-NSAF. This algorithm has faster convergence speed than L_0 -NSAF for BS system identification.
- Establishment of the BS-IMSAF. The BS-IMSAF has better convergence speed than BS-NSAF.
- Introducing the BS-DSR-IMSAF and BS-SR-IMSAF algorithms. These algorithms have lower computational complexity than BS-IMSAF.
- Studying the theoretical steady-state performance of proposed algorithms.
- Demonstrating of the proposed algorithms through several simulation results.

This paper is organized as follows: Sect. 2 describes the data model and IMSAF algorithm. In Sect. 3, the IMSAF is derived based on the gradient descent approach. In Sect. 4, the BS-NSAF algorithm is introduced. The family of BS-

IMSAF is proposed in 5. Sect. 6 studies the theoretical steady-state performance of the algorithms. The computational complexity of the proposed algorithm is discussed in Sect. 7. Finally, the paper ends with a comprehensive set of simulations supporting the validity of the results.

Throughout the paper, $(\cdot)^T$ represents transpose of a vector or matrix, $\|\cdot\|_0$ indicates ℓ_0 -norm of a vector, $\|\cdot\|^2$ takes the squared Euclidean norm of a vector, $\|\cdot\|_{2,0}$ creates $L_{2,0}$ -norm of a vector, $\lceil \cdot \rceil$ describes the Ceiling function, and $E\{\cdot\}$ shows the Expectation.

Data Model and Review of IMSAF Algorithm

Consider a linear data model for the desired signal as

$$d(k) = \mathbf{u}^T(k) \mathbf{h}^0 + v(k), \quad (1)$$

where \mathbf{h}^0 is an unknown M -dimensional filter coefficients that we want to estimate, $v(k)$ is the additive noise with variance σ_v^2 , and $\mathbf{u}(k) = [u(k), u(k-1), \dots, u(k-M+1)]^T$ denotes an M -dimensional input regressor vector. It is assumed that $v(k)$ is zero mean, white, Gaussian, and independent of $\mathbf{u}(k)$.

Fig. 1 shows the structure of the NSAF [7]. In this figure, $\mathbf{f}_1, \mathbf{f}_2, \dots, \mathbf{f}_N$ and $\mathbf{g}_1, \mathbf{g}_2, \dots, \mathbf{g}_N$, are analysis and synthesis filter impulse responses of N channel. The $u_i(k)$ and $d_i(k)$ are nondecimated subband signals. It is important to note that k refers to the index of the original sequences and n denotes the index of the decimated sequences ($n = \text{floor}(k/N)$). The decimated output signal is defined as $y_{i,D}(n) = \mathbf{u}_i^T(n) \mathbf{h}(n)$, $\mathbf{h}(n) = [h_1(n), h_2(n), \dots, h_M(n)]^T$ and $\mathbf{u}_i(n) = [u_i(nN), u_i(nN-1), \dots, u_i(nN-M+1)]^T$. Also, the decimated subband error signal is expressed as $e_{i,D}(n) = d_{i,D}(n) - \mathbf{u}_i^T(n) \mathbf{h}(n)$.

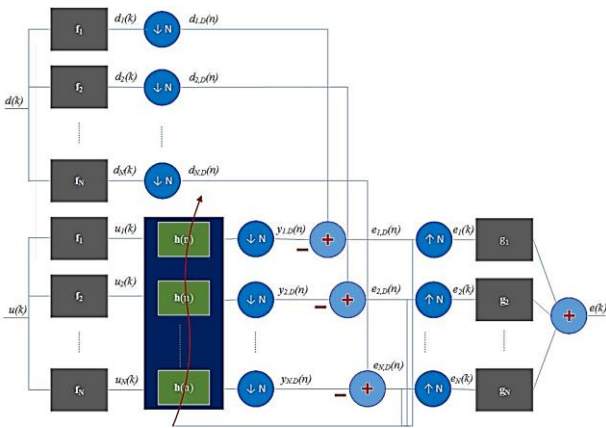


Fig. 1: Structure of the NSAF algorithm.

Now, by defining $[\mathbf{U}_i(n)]_{M \times K}$ and $[\mathbf{d}_{i,D}(n)]_{K \times 1}$ as

$$\mathbf{U}_i(n) = [\mathbf{u}_i(n), \mathbf{u}_i(n-1), \dots, \mathbf{u}_i(n-K+1)], \quad (2)$$

$$\mathbf{d}_{i,D}(n) = [d_{i,D}(n), \dots, d_{i,D}(n-K+1)]^T, \quad (3)$$

the IMSAF algorithm is derived from the solution of the following constraint optimization problem [12], [13],

$$J(n) = \|\mathbf{h}(n+1) - \mathbf{h}(n)\|^2 + \sum_{i=1}^N \Lambda_i [\mathbf{d}_{i,D}(n) - \mathbf{U}_i^T(n) \mathbf{h}(n+1)], \quad (4)$$

where $\Lambda_i = [\lambda_{i,1}, \lambda_{i,2}, \dots, \lambda_{i,K}]$ is the Lagrange multipliers vector with length K . Using $\frac{\partial J(n)}{\partial \mathbf{h}(n+1)} = 0$ and $\frac{\partial J(n)}{\partial \Lambda_i} = 0$, we get

$$\mathbf{h}(n+1) = \mathbf{h}(n) + \frac{1}{2} \sum_{i=1}^N \mathbf{U}_i(n) \Lambda_i^T, \quad (5)$$

where

$$\Lambda_i^T = 2[\mathbf{U}_i^T(n) \mathbf{U}_i(n)]^{-1} \mathbf{e}_{i,D}(n), \quad (6)$$

and the output error vector, $[\mathbf{e}_{i,D}(n)]_{K \times 1}$, is given by

$$\mathbf{e}_{i,D}(n) = \mathbf{d}_{i,D}(n) - \mathbf{U}_i^T(n) \mathbf{h}(n), \quad (7)$$

Therefore, the update equation for IMSAF becomes

$$\mathbf{h}(n+1) = \mathbf{h}(n) + \mu \sum_{i=1}^N \mathbf{U}_i(n) [\mathbf{U}_i^T(n) \mathbf{U}_i(n)]^{-1} \mathbf{e}_{i,D}(n), \quad (8)$$

where μ is the step-size.

Derivation of IMSAF Based on the Gradient Descent Method

In this section, we establish the IMSAF algorithm based on the gradient descent approach. Instead of minimizing (4), the following cost function is defined as [29].

$$J(n) = \frac{1}{2} \sum_{i=1}^N \mathbf{e}_{i,D}^T(n) [\mathbf{U}_i^T(n) \mathbf{U}_i(n)]^{-1} \mathbf{e}_{i,D}(n), \quad (9)$$

Based on the gradient descent approach, the filter coefficients recursion is given by

$$\mathbf{h}(n+1) = \mathbf{h}(n) - \mu \frac{\partial J(n)}{\partial \mathbf{h}(n)}, \quad (10)$$

Using (7) in (9), $J(n)$ becomes

$$J(n) = \frac{1}{2} \sum_{i=0}^{N-1} \{ \mathbf{d}_{i,D}^T(n) [\mathbf{U}_i^T(n) \mathbf{U}_i(n)]^{-1} \mathbf{d}_{i,D}(n) + 2 \mathbf{h}^T(n) \mathbf{U}_i(n) [\mathbf{U}_i^T(n) \mathbf{U}_i(n)]^{-1} \mathbf{d}_{i,D}(n) + \mathbf{h}^T(n) \mathbf{U}_i(n) [\mathbf{U}_i^T(n) \mathbf{U}_i(n)]^{-1} \mathbf{U}_i^T(n) \mathbf{h}(n) \}, \quad (11)$$

and the gradient of $J(n)$ is

$$\begin{aligned} \frac{\partial J(n)}{\partial \mathbf{h}(n)} &= \sum_{i=1}^N \{ -\mathbf{U}_i(n) [\mathbf{U}_i^T(n) \mathbf{U}_i(n)]^{-1} \mathbf{d}_{i,D}(n) \\ &\quad + \mathbf{U}_i(n) [\mathbf{U}_i^T(n) \mathbf{U}_i(n)]^{-1} \mathbf{U}_i^T(n) \mathbf{h}(n) \} \\ &= -\sum_{i=1}^N \{ \mathbf{U}_i(n) [\mathbf{U}_i^T(n) \mathbf{U}_i(n)]^{-1} \mathbf{e}_{i,D}(n) \}, \end{aligned} \quad (12)$$

By substituting (12) in (10), the IMSAF algorithm is established as

$$\begin{aligned} \mathbf{h}(n+1) &= \mathbf{h}(n) + \mu \sum_{i=1}^N \mathbf{U}_i(n) [\mathbf{U}_i^T(n) \mathbf{U}_i(n)]^{-1} \mathbf{e}_{i,D}(n), \end{aligned} \quad (13)$$

Review of BS-LMS and derivation of BS-NSAF

In this section, we briefly review BS-LMS adaptive algorithms [27]. Then, the BS-NSAF is introduced.

A. Review of BS-LMS algorithm

In BS-LMS, a penalty of block-sparsity is inserted to the cost function of traditional LMS algorithms. This penalty is a mixed of $L_{2,0}$ -norm of adaptive filter coefficients with equal group partition sizes. In BS-LMS, the cost function is defined as [27].

$$J(k) = |e(k)|^2 + \delta \| \mathbf{h}(k) \|_{2,0}, \quad (14)$$

where δ is positive factor to balance the estimation error and the penalty of block-sparsity. Also

$$\| \mathbf{h}(k) \|_{2,0} \approx \left\| \begin{matrix} \| \mathbf{h}_{[1]} \|_2 \\ \| \mathbf{h}_{[2]} \|_2 \\ \vdots \\ \| \mathbf{h}_{[B]} \|_2 \end{matrix} \right\|_0, \quad (15)$$

and

$$\mathbf{h}_{[i]} = [h_{(i-1)L+1}, h_{(i-1)L+2}, \dots, h_{iL}]^T, \quad (16)$$

Denotes the i th block of \mathbf{h} . The parameters B and L are the number of blocks and the block partition size, respectively. Following the same strategy in L_0 -LMS [18], the update equation for BS-LMS is given by

$$\mathbf{h}(k+1) = \mathbf{h}(k) + \mu e(k) \mathbf{u}(k) + \kappa \mathbf{f}(\mathbf{h}(k)), \quad (17)$$

where $\kappa = \mu\delta$ regulates the strength of block-sparse penalty for given step-size and zero attraction function

$$\mathbf{f}(\mathbf{h}(k)) = [f_1(\mathbf{h}(k)), f_2(\mathbf{h}(k)), \dots, f_M(\mathbf{h}(k))]^T, \quad (18)$$

$$f_j(\mathbf{h}(k)) = \begin{cases} \gamma^2 h_j(k) - \frac{\gamma h_j(k)}{\| \mathbf{h}_{[j/L]} \|_2}, \\ \text{when } 0 < \| \mathbf{h}_{[j/L]} \|_2 \leq \frac{1}{\gamma}, \\ 0, & \text{otherwise.} \end{cases} \quad (19)$$

Fig. 2 shows zero attraction function for BS-LMS when $\gamma = 1$ and different length of blocks, $L = 1, 2, 4, 8$.

If we have one block in BS-LMS, $L = 1$, then the zero attraction function in BS-LMS reduces to the zero attraction function in L_0 -LMS. Zero attraction imposes an attraction to zero on small weight coefficients. After each iteration, a filter weight will decrease a little when it is positive, or increase a little when it is negative. Therefore, it seems that in space of weight coefficients, an attractor, which attracts the nonzero vectors, exists at the coordinate origin. The function of zero attractor improves the performance of LMS in sparse system identification. To be specific, in the adaptation process, a weight coefficient closer to zero shows a higher possibility of being zero itself in the impulse response.

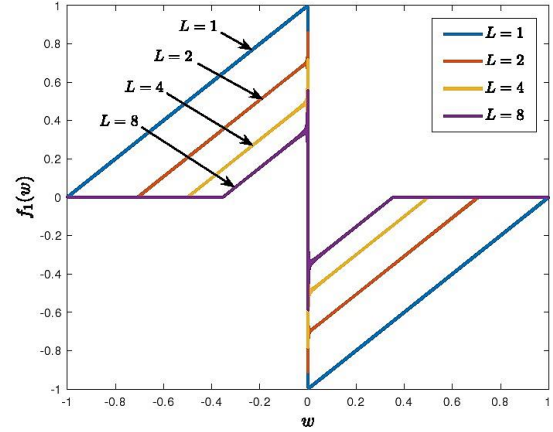


Fig. 2: Zero attraction function for BS-LMS when $\gamma=1, L=1,2,4,8$.

B. Proposed BS-NSAF algorithm

In [19], the L_0 -NSAF was proposed. To improve the performance of NSAF and L_0 -NSAF for block-sparse system identification, the BS-NSAF is presented. If the parameter K in (8) is set to 1, the NSAF algorithm is established. Therefore, by selecting this value in (9), the cost function for BS-NSAF algorithm is proposed as

$$J(n) = \frac{1}{2} \sum_{i=1}^N \frac{|e_{i,D}(n)|^2}{\| \mathbf{u}_i(n) \|^2} + \delta \| \mathbf{h}(n) \|_{2,0}, \quad (20)$$

Now, by applying the gradient descent approach in (10) to the proposed cost function and setting $\frac{\partial J(n)}{\partial \mathbf{h}(n)}$ equal to zero, we get

$$\frac{\partial J(n)}{\partial \mathbf{h}(n)} = - \sum_{i=1}^N \frac{\mathbf{u}_i(n) e_{i,D}(n)}{\| \mathbf{u}_i(n) \|^2} + \delta \frac{\partial \| \mathbf{h}(n) \|_{2,0}}{\partial \mathbf{h}(n)}, \quad (21)$$

Finally, the update equation for BS-NSAF is established as

$$\mathbf{h}(n+1) = \mathbf{h}(n) + \mu \sum_{i=1}^N \frac{\mathbf{u}_i(n) e_{i,D}(n)}{\| \mathbf{u}_i(n) \|^2} + \kappa \mathbf{f}(\mathbf{h}(n)), \quad (22)$$

where

$$\mathbf{f}(\mathbf{h}(n)) = [f_1(\mathbf{h}(n)), f_2(\mathbf{h}(n)), \dots, f_M(\mathbf{h}(n))]^T, \quad (23)$$

The Family of BS-IMSAF Algorithms

Although, the IMSAF works well for dispersive unknown systems, its performance needs to be improved when the impulse response is block-sparse. In this section, three block-sparse adaptive algorithms are proposed. The first algorithm is BS-IMSAF algorithm. In the following, to reduce the computational complexity of BS-IMSAF algorithm, the selective regressors (SR) and dynamic selection of regressors (DSR) strategies are utilized and BS-SR-IMSAF and BS-DSR-IMSAF algorithms are derived.

A. The BS-IMSAF algorithm

By applying $L_{2,0}$ -norm into (9), the optimization problem turns to

$$J(n) = \frac{1}{2} \sum_{i=1}^N \mathbf{e}_{i,D}^T(n) [\mathbf{U}_i^T(n) \mathbf{U}_i(n)]^{-1} \mathbf{e}_{i,D}(n) + \delta \|\mathbf{h}(n)\|_{2,0}, \quad (24)$$

Setting $\frac{\partial J(n)}{\partial \mathbf{h}(n)}$ equal to zero,

$$\frac{\partial J(n)}{\partial \mathbf{h}(n)} = - \sum_{i=1}^N \{ \mathbf{U}_i(n) [\mathbf{U}_i^T(n) \mathbf{U}_i(n)]^{-1} \mathbf{e}_{i,D}(n) \} + \delta \frac{\partial \|\mathbf{h}(n)\|_{2,0}}{\partial \mathbf{h}(n)}, \quad (25)$$

the weight coefficients update equation becomes

$$\mathbf{h}(n+1) = \mathbf{h}(n) - \mu \delta \frac{\partial \|\mathbf{h}(n)\|_{2,0}}{\partial \mathbf{h}(n)} + \mu \sum_{i=1}^N \mathbf{U}_i(n) [\mathbf{U}_i^T(n) \mathbf{U}_i(n)]^{-1} \mathbf{e}_{i,D}(n), \quad (26)$$

Finally, the weight update equation for BS-IMSAF is described as

$$\mathbf{h}(n+1) = \mathbf{h}(n) + \kappa \mathbf{f}(\mathbf{h}(n)) + \mu \sum_{i=1}^N \mathbf{U}_i(n) [\mathbf{U}_i^T(n) \mathbf{U}_i(n)]^{-1} \mathbf{e}_{i,D}(n), \quad (27)$$

where $\mathbf{f}(\mathbf{h}(n))$ is obtained from (24) and (25). Table 3 summarizes the BS-IMSAF algorithm.

Table 3: The BS-IMSAF algorithm

For $n = 0, 1, \dots$

$$\mathbf{u}(n) = [u(n), u(n-1), \dots, u(n-M+1)]^T$$

For $i = 1, \dots, N$

$$\mathbf{d}_{i,D}(n) = [d_{i,D}(n), \dots, d_{i,D}(n-K+1)]^T$$

$$\mathbf{U}_i(n) = [\mathbf{u}_i(n), \mathbf{u}_i(n-1), \dots, \mathbf{u}_i(n-K+1)]$$

$$\mathbf{e}_{i,D}(n) = \mathbf{d}_{i,D}(n) - \mathbf{U}_i^T(n) \mathbf{h}(n)$$

End

%—Update the filter:

$$\mathbf{f}(\mathbf{h}(n)) = [f_1(\mathbf{h}(n)), f_2(\mathbf{h}(n)), \dots, f_M(\mathbf{h}(n))]^T$$

$$f_j(\mathbf{h}(n)) = \begin{cases} \gamma^2 h_j(n) - \frac{\gamma h_j(n)}{\|\mathbf{h}_{[j/L]}(n)\|_2}, \\ \text{when } 0 < \|\mathbf{h}_{[j/L]}(n)\|_2 \leq \frac{1}{\gamma}, \\ 0, & \text{otherwise.} \end{cases}$$

$$\mathbf{h}(n+1) = \mathbf{h}(n) + \kappa \mathbf{f}(\mathbf{h}(n)) + \mu \sum_{i=1}^N \mathbf{U}_i(n) [\mathbf{U}_i^T(n) \mathbf{U}_i(n) + \epsilon \mathbf{I}]^{-1} \mathbf{e}_{i,D}(n)$$

End

B. The BS-SR-IMSAF Algorithm

In BS-SR-IMSAF, a subset of the input regressors at each subband is optimally selected for every adaptation. Let $\Theta_S = \{\theta_1, \theta_2, \dots, \theta_S\}$ denotes a S -subsets (subsets with S members) of the $\{0, 1, \dots, K-1\}$. Now define

$$\mathbf{d}_{i,D,\Theta_S}(n) = [d_{i,D}(n-\theta_1), \dots, d_{i,D}(n-\theta_S)]^T, \quad (28)$$

and

$$\mathbf{U}_{i,\Theta_S}(n) = [\mathbf{u}_i(n-\theta_1), \dots, \mathbf{u}_i(n-\theta_S)], \quad (29)$$

Therefore, the output error vector is given by

$$\mathbf{e}_{i,D,\Theta_S}(n) = \mathbf{d}_{i,D,\Theta_S}(n) - \mathbf{U}_{i,\Theta_S}^T(n) \mathbf{h}(n), \quad (30)$$

The cost function for BS-SR-IMSAF is defined as

$$J_{\Theta_S}(n) = \delta \|\mathbf{h}(n)\|_{2,0} + \frac{1}{2} \sum_{i=1}^N \mathbf{e}_{i,D,\Theta_S}^T(n) [\mathbf{U}_{i,\Theta_S}^T(n) \mathbf{U}_{i,\Theta_S}(n)]^{-1} \mathbf{e}_{i,D,\Theta_S}(n). \quad (31)$$

Following the same approach in BS-IMSAF, we get

$$\mathbf{h}(n+1) = \mathbf{h}(n) + \kappa \mathbf{f}(\mathbf{h}(n)) + \mu \sum_{i=1}^N \mathbf{U}_{i,\Theta_S}(n) [\mathbf{U}_{i,\Theta_S}^T(n) \mathbf{U}_{i,\Theta_S}(n)]^{-1} \mathbf{e}_{i,D,\Theta_S}(n), \quad (32)$$

We should select the regressors which makes $J_{\Theta_S}(n)$ as close as possible to $J(n)$. Thus, the optimum selection of the input regressors is obtained by a subset that minimizes

$$\Theta_S^{opt} = \left| \sum_{i=1}^N [\mathbf{e}_{i,D}^T(n) (\mathbf{U}_i^T(n) \mathbf{U}_i(n))^{-1} \mathbf{e}_{i,D}(n) - \mathbf{e}_{i,D,\Theta_S}^T(n) (\mathbf{U}_{i,\Theta_S}^T(n) \mathbf{U}_{i,\Theta_S}(n))^{-1} \mathbf{e}_{i,D,\Theta_S}(n)] \right|, \quad (33)$$

Since $\mathbf{e}_{i,D,\Theta_S}^T(n) (\mathbf{U}_{i,\Theta_S}^T(n) \mathbf{U}_{i,\Theta_S}(n))^{-1} \mathbf{e}_{i,D,\Theta_S}(n)$ is always smaller than $\mathbf{e}_{i,D}^T(n) (\mathbf{U}_i^T(n) \mathbf{U}_i(n))^{-1} \mathbf{e}_{i,D}(n)$, the optimum selection is reformulated by a subset that maximizes

$$\Theta_S^{opt} = \sum_{i=1}^N [\mathbf{e}_{i,D,\Theta_S}^T(n) (\mathbf{U}_{i,\Theta_S}^T(n) \mathbf{U}_{i,\Theta_S}(n))^{-1} \mathbf{e}_{i,D,\Theta_S}(n)], \quad (34)$$

To reduce the computational complexity of (36), we assume that the diagonal elements of $\mathbf{U}_{i,\Theta_S}^T(n) \mathbf{U}_{i,\Theta_S}(n)$ is much larger than off-diagonal elements [10], [12]. Therefore, (34) is approximated for each subband as

$$\mathbf{e}_{i,D,\Theta_S}^T(n) (\mathbf{U}_{i,\Theta_S}^T(n) \mathbf{U}_{i,\Theta_S}(n))^{-1} \mathbf{e}_{i,D,\Theta_S}(n) \approx \frac{e_{i,D}^2(n-\theta_1)}{\|\mathbf{u}_i(n-\theta_1)\|^2} + \dots + \frac{e_{i,D}^2(n-\theta_S)}{\|\mathbf{u}_i(n-\theta_S)\|^2}, \quad (35)$$

where $\mathbf{e}_{i,D}(n) = [e_{i,D}(n), e_{i,D}(n-1), \dots, e_{i,D}(n-K+1)]^T$. Based on (35), the indices of the optimum subset at each subband for every iteration are obtained by the following simplified procedure:

1. Compute the following values for $0 \leq j \leq K-1$ and $1 \leq i \leq N$

$$\frac{e_{i,D}^2(n-j)}{\|\mathbf{u}_i(n-j)\|^2}, \quad (36)$$

2. The j -indices of Θ_s^{opt} for each i correspond to the indices of the S largest values of (36).

The BS-DSR-IMSAF Algorithm

In BS-DSR-IMSAF, the number of selected input regressors at each subband are dynamically changed for every adaptation. By defining the weight error vector as $\tilde{\mathbf{h}}(n) = \mathbf{h}^o - \mathbf{h}(n)$, the weight error vector update equation in BS-IMSAF can be stated as

$$\begin{aligned} \tilde{\mathbf{h}}(n+1) &= \tilde{\mathbf{h}}(n) - \kappa \mathbf{f}(\mathbf{h}(n)) \\ &\quad - \mu \sum_{i=1}^N \mathbf{U}_i(n) [\mathbf{U}_i^T(n) \mathbf{U}_i(n)]^{-1} \mathbf{e}_{i,D}(n), \end{aligned} \quad (37)$$

Table 4 summarizes the BS-SR-IMSAF algorithm.

Table 4: The BS-SR-IMSAF algorithm

For $n = 0, 1, \dots$
 $\mathbf{u}(n) = [u(n), u(n-1), \dots, u(n-M+1)]^T$

For $i = 1, \dots, N$
 $\mathbf{d}_{i,D}(n) = [d_{i,D}(n), \dots, d_{i,D}(n-K+1)]^T$
 $\mathbf{U}_i(n) = [\mathbf{u}_i(n), \mathbf{u}_i(n-1), \dots, \mathbf{u}_i(n-K+1)]$
 $\mathbf{e}_{i,D}(n) = \mathbf{d}_{i,D}(n) - \mathbf{U}_i^T(n) \mathbf{h}(n)$

%—Determining the s -indices:
 For $j = 0, 1, \dots, K-1$
 compute $\frac{e_{i,D}^2(n-j)}{\|\mathbf{u}_i(n-j)\|^2}$
 End

%—Update the desired signal vector:
 $\mathbf{U}_{i,\Theta_s}(n) = [\mathbf{u}_i(n-\theta_1), \dots, \mathbf{u}_i(n-\theta_S)]$
 $\mathbf{d}_{i,D,\Theta_s}(n) = [d_{i,D}(n-\theta_1), \dots, d_{i,D}(n-\theta_S)]^T$
 $\mathbf{e}_{i,D,\Theta_s}(n) = \mathbf{d}_{i,D,\Theta_s}(n) - \mathbf{U}_{i,\Theta_s}^T(n) \mathbf{h}(n)$
 End

%—Update the filter:
 $\mathbf{f}(\mathbf{h}(n)) = [f_1(\mathbf{h}(n)), f_2(\mathbf{h}(n)), \dots, f_M(\mathbf{h}(n))]^T$

$$f_j(\mathbf{h}(n)) = \begin{cases} \gamma^2 h_j(n) - \frac{\gamma h_j(n)}{\|\mathbf{h}_{[j/L]}\|_2}, \\ \text{when } 0 < \|\mathbf{h}_{[j/L]}\|_2 \leq \frac{1}{\gamma}, \\ 0, & \text{otherwise.} \end{cases}$$

 $\mathbf{h}(n+1) = \mathbf{h}(n) + \kappa \mathbf{f}(\mathbf{h}(n)) + \mu \sum_{i=1}^N \{\mathbf{U}_{i,\Theta_s}(n) \times [\mathbf{U}_{i,\Theta_s}^T(n) \mathbf{U}_{i,\Theta_s}(n) + \epsilon \mathbf{I}]^{-1} \mathbf{e}_{i,D,\Theta_s}(n)\}$
 End

Taking the squared Euclidean norm and then expectation from both sides of (39) leads to the mean-square deviation (MSD) that satisfies

$$E \|\tilde{\mathbf{h}}(n+1)\|^2 = E \|\tilde{\mathbf{h}}(n)\|^2 - \Delta, \quad (38)$$

where

$$\begin{aligned} \Delta &= \sum_{i=1}^N [\mu(2-\mu) E \{ \mathbf{e}_{i,D}^T(n) (\mathbf{U}_i^T(n) \mathbf{U}_i(n))^{-1} \mathbf{e}_{i,D}(n) \} \\ &\quad - 2\mu \sigma_{v_{i,D}}^2 \text{Tr}(E[\mathbf{U}_i^T(n) \mathbf{U}_i(n)]^{-1})] \\ &\quad + \{\text{crosstermswith}\kappa\}, \end{aligned} \quad (39)$$

If Δ is maximized, then the fastest convergence is obtained. In (39), $\sigma_{v_{i,D}}^2$ is the variance of the i th subband signal of $v_i(n)$ being partitioned and decimated. We assume that the $\{\text{crosstermof}\kappa\}$ are zero, because κ is very small value. Since the exact expected values are not available, the instantaneous values are used as follows

$$\begin{aligned} \hat{\Delta} &= \mu(2-\mu) \sum_{i=1}^N [\mathbf{e}_{i,D}^T(n) (\mathbf{U}_i^T(n) \mathbf{U}_i(n))^{-1} \mathbf{e}_{i,D}(n) \\ &\quad - \frac{2}{2-\mu} \sigma_{v_{i,D}}^2 \text{Tr}[\mathbf{U}_i^T(n) \mathbf{U}_i(n)]^{-1}], \end{aligned} \quad (40)$$

Again we use the previous approximation for $\mathbf{U}_i^T(n) \mathbf{U}_i(n)$ and obtain [11], [12]

$$\begin{aligned} \hat{\Delta} &= \mu(2-\mu) \sum_{i=1}^N \left\{ \left(\frac{e_{i,D}^2(n) - 2\sigma_{v_{i,D}}^2/(2-\mu)}{\|\mathbf{u}_i(n)\|^2} \right) \right. \\ &\quad \left. + \left(\frac{e_{i,D}^2(n-1) - 2\sigma_{v_{i,D}}^2/(2-\mu)}{\|\mathbf{u}_i(n-1)\|^2} \right) + \dots \right. \\ &\quad \left. + \left(\frac{e_{i,D}^2(n-P+1) - 2\sigma_{v_{i,D}}^2/(2-\mu)}{\|\mathbf{u}_i(n-K+1)\|^2} \right) \right\}, \end{aligned} \quad (41)$$

From (41), we can find the following facts. If at each subband $e_{i,D}^2(n-j) > 2\sigma_{v_{i,D}}^2/(2-\mu)$, then $\mathbf{u}_i(n-j)$ contributes to maximizing $\hat{\Delta}$. However, if $e_{i,D}^2(n-j) \leq 2\sigma_{v_{i,D}}^2/(2-\mu)$, then $\mathbf{u}_i(n-j)$ makes $\hat{\Delta}$ decrease. Therefore, we should perform the update with the input regressors satisfying $e_{i,D}^2(n-j) > 2\sigma_{v_{i,D}}^2/(2-\mu)$ at every iteration for the largest MSD decrease. Thus, the number of the selected input regressors at each subband for every iteration should be the same as the number of errors satisfying $e_{i,D}^2(n-j) > 2\sigma_{v_{i,D}}^2/(2-\mu)$.

Suppose $\Theta_{S_i(n)} = \{\theta_1, \theta_2, \dots, \theta_{S_i(n)}\}$ indicates a subset with $S_i(n)$ members of the set $\{0, 1, \dots, K-1\}$ at each subband. Then, the update equation for proposed BS-DSR-IMSAF is introduced as

$$\begin{aligned} \mathbf{h}(n+1) &= \mathbf{h}(n) + \kappa \mathbf{f}(\mathbf{h}(n)) + \mu \sum_{i=1}^N \mathbf{U}_{i,\Theta_{S_i(n)}}(n) \\ &\quad [\epsilon \mathbf{I} + \mathbf{U}_{i,\Theta_{S_i(n)}}^T(n) \mathbf{U}_{i,\Theta_{S_i(n)}}(n)]^{-1} \mathbf{e}_{i,D,\Theta_{S_i(n)}}(n), \end{aligned} \quad (42)$$

where

$$\mathbf{d}_{i,D,\Theta_{S_i(n)}}(n) = [d_{i,D}(n-\theta_1), \dots, d_{i,D}(n-\theta_{S_i(n)})]^T, \quad (43)$$

$$\mathbf{U}_{i,\Theta_{S_i(n)}}(n) = [\mathbf{u}_i(n-\theta_1), \dots, \mathbf{u}_i(n-\theta_{S_i(n)})], \quad (44)$$

and

$$\mathbf{e}_{i,D,\theta_{S_i(n)}}(n) = \mathbf{d}_{i,D,\theta_{S_i(n)}}(n) - \mathbf{U}_{i,\theta_{S_i(n)}}^T(n)\mathbf{h}(n). \quad (45)$$

The parameter $S_i(n)$ changes between 0 and K . The indices of the subset ($J_{S_i(n)}$) are obtained through the following procedure:

1. Compute the following values for $0 \leq j \leq K - 1$ and $0 \leq i \leq N - 1$

$$|e_{i,D}(n-j)| > \sqrt{\frac{2}{2-\mu}} \sigma_{v_{i,D}}, \quad (46)$$

2. The j -indices of $J_{S_i(n)}$ at each subband correspond to the indices that satisfies the condition in (46).

Table 5 summarizes the BS-DSR-IMSAF algorithm.

Table 5: The BS-DSR-IMSAF algorithm

For $n = 0, 1, \dots$
$\mathbf{u}(n) = [u(n), u(n-1), \dots, u(n-M+1)]^T$
For $i = 1, \dots, N$
$\mathbf{d}_{i,D}(n) = [d_{i,D}(n), \dots, d_{i,D}(n-K+1)]^T$
$\mathbf{U}_i(n) = [\mathbf{u}_i(n), \mathbf{u}_i(n-1), \dots, \mathbf{u}_i(n-K+1)]$
$\mathbf{e}_{i,D}(n) = \mathbf{d}_{i,D}(n) - \mathbf{U}_i^T(n)\mathbf{h}(n)$
%—Determining the s -indices:
For $j = 0, 1, \dots, K - 1$
compute $ e_{i,D}(n-j) > \sqrt{\frac{2}{2-\mu}} \sigma_{v_{i,D}}$
End
%—Update the desired signal vector:
$\mathbf{U}_{i,\theta_{S_i(n)}}(n) = [\mathbf{u}_i(n - \theta_1), \dots, \mathbf{u}_i(n - \theta_{S_i(n)})]$
$\mathbf{d}_{i,D,\theta_{S_i(n)}}(n) = [d_{i,D}(n - \theta_1), \dots, d_{i,D}(n - \theta_{S_i(n)})]^T$
$\mathbf{e}_{i,D,\theta_{S_i(n)}}(n) = \mathbf{d}_{i,D,\theta_{S_i(n)}}(n) - \mathbf{U}_{i,\theta_{S_i(n)}}^T(n)\mathbf{h}(n)$.
End
%—Update the filter:
$\mathbf{f}(\mathbf{h}(n)) = [f_1(\mathbf{h}(n)), f_2(\mathbf{h}(n)), \dots, f_M(\mathbf{h}(n))]^T$
$f_j(\mathbf{h}(n)) = \begin{cases} \gamma^2 h_j(n) - \frac{\gamma h_j(n)}{\ \mathbf{h}_{[j/L]}\ _2}, \\ \text{when } 0 < \ \mathbf{h}_{[j/L]}\ _2 \leq \frac{1}{\gamma}, \\ 0, \quad \text{otherwise.} \end{cases}$
$\mathbf{h}(n+1) = \mathbf{h}(n) + \kappa \mathbf{f}(\mathbf{h}(n)) + \mu \sum_{i=1}^N \{\mathbf{U}_{i,\theta_{S_i(n)}}(n) \times [\epsilon \mathbf{I} + \mathbf{U}_{i,\theta_{S_i(n)}}^T(n)\mathbf{U}_{i,\theta_{S_i(n)}}(n)]^{-1} \mathbf{e}_{i,D,\theta_{S_i(n)}}(n)\}$
End

Theoretical Performance Analysis

In this section, we analyze the performance of the family of BS-IMSAF algorithms. By defining the weight error vector, $\tilde{\mathbf{h}} = \mathbf{h}^o - \mathbf{h}(n)$, the general weight error vector update equation can be written as

$$\begin{aligned} \tilde{\mathbf{h}}(n+1) &= \tilde{\mathbf{h}}(n) - \kappa \mathbf{f}(\mathbf{h}(n)) \\ &\quad - \mu \sum_{i=0}^{N-1} \mathbf{U}_i(n) [\mathbf{U}_i^T(n)\mathbf{U}_i(n)]^{-1} \mathbf{e}_{i,D}(n), \end{aligned} \quad (47)$$

where $\mathbf{U}_i(n)$ and $\mathbf{e}_{i,D}(n)$ is defined according to the Table 6.

Table 6: The definitions of $\mathbf{U}_i(n)$ and $\mathbf{e}_{i,D}(n)$

Algorithm	$\mathbf{U}_i(n)$	$\mathbf{e}_{i,D}(n)$
BS-IMSAF	$\mathbf{U}_i(n)$	$\mathbf{e}_{i,D}(n)$
BS-SR-IMSAF	$\mathbf{U}_{i,\theta_S}(n)$	$\mathbf{e}_{i,D,\theta_S}(n)$
BS-DSR-IMSAF	$\mathbf{U}_{i,\theta_{S_i(n)}}(n)$	$\mathbf{e}_{i,D,\theta_{S_i(n)}}(n)$

By taking the squared Euclidean norm from both sides of (25), we get

$$\|\tilde{\mathbf{h}}(n+1)\|^2 = \|\tilde{\mathbf{h}}(n)\|^2, \quad (48)$$

$$\begin{aligned} &-2\mu \sum_{i=0}^{N-1} [\tilde{\mathbf{h}}^T(n)\mathbf{U}_i(n)(\mathbf{U}_i^T(n)\mathbf{U}_i(n))^{-1} \mathbf{e}_{i,D}(n) \\ &+ 2\mu\kappa \sum_{i=0}^{N-1} [\mathbf{f}^T(\mathbf{h}(n))\mathbf{U}_i(n)(\mathbf{U}_i^T(n)\mathbf{U}_i(n))^{-1} \mathbf{e}_{i,D}(n) \\ &+ \mu^2 \sum_{i=0}^{N-1} \mathbf{e}_{i,D}^T(n)(\mathbf{U}_i^T(n)\mathbf{U}_i(n))^{-1} \mathbf{e}_{i,D}(n) \\ &\quad - \kappa \mathbf{f}^T(\mathbf{h}(n))\tilde{\mathbf{h}}(n) + \kappa^2 \|\mathbf{f}(\mathbf{h}(n))\|^2], \end{aligned} \quad (49)$$

From (1) and (7), we have

$$\tilde{\mathbf{h}}^T(n)\mathbf{U}_i(n) = \mathbf{e}_{i,D}^T(n) - \mathbf{v}_{i,D}^T(n), \quad (50)$$

Therefore, (49) is reformulated as

$$\begin{aligned} &\|\tilde{\mathbf{h}}(n+1)\|^2 = \|\tilde{\mathbf{h}}(n)\|^2 \\ &-2\mu \sum_{i=0}^{N-1} [\mathbf{e}_{i,D}^T(n) - \mathbf{v}_{i,D}^T(n)] (\mathbf{U}_i^T(n)\mathbf{U}_i(n))^{-1} \mathbf{e}_{i,D}(n) \\ &+ 2\mu\kappa \sum_{i=0}^{N-1} \mathbf{f}^T(\mathbf{h}(n))\mathbf{U}_i(n)(\mathbf{U}_i^T(n)\mathbf{U}_i(n))^{-1} \mathbf{e}_{i,D}(n) \\ &+ \mu^2 \sum_{i=0}^{N-1} \mathbf{e}_{i,D}^T(n)(\mathbf{U}_i^T(n)\mathbf{U}_i(n))^{-1} \mathbf{e}_{i,D}(n) \\ &\quad - \kappa \mathbf{f}^T(\mathbf{h}(n))\tilde{\mathbf{h}}(n) + \kappa^2 \|\mathbf{f}(\mathbf{h}(n))\|^2, \end{aligned} \quad (51)$$

which can be stated as

$$\begin{aligned} &\|\tilde{\mathbf{h}}(n+1)\|^2 = \|\tilde{\mathbf{h}}(n)\|^2 \\ &\quad - 2\mu \sum_{i=0}^{N-1} \mathbf{e}_{i,D}^T(n)(\mathbf{U}_i^T(n)\mathbf{U}_i(n))^{-1} \mathbf{e}_{i,D}(n) \\ &\quad + 2\mu \sum_{i=0}^{N-1} \mathbf{v}_{i,D}^T(n)(\mathbf{U}_i^T(n)\mathbf{U}_i(n))^{-1} \mathbf{e}_{i,D}(n) \\ &+ 2\mu\kappa \sum_{i=0}^{N-1} \mathbf{f}^T(\mathbf{h}(n))\mathbf{U}_i(n)(\mathbf{U}_i^T(n)\mathbf{U}_i(n))^{-1} \mathbf{e}_{i,D}(n) \\ &+ \mu^2 \sum_{i=0}^{N-1} \mathbf{e}_{i,D}^T(n)(\mathbf{U}_i^T(n)\mathbf{U}_i(n))^{-1} \mathbf{e}_{i,D}(n) \\ &\quad - \kappa \mathbf{f}^T(\mathbf{h}(n))\tilde{\mathbf{h}}(n) + \kappa^2 \|\mathbf{f}(\mathbf{h}(n))\|^2, \end{aligned} \quad (52)$$

To simplify the recent relation, we apply the following independence assumptions [12], [30]:

1. $\mathbf{U}_i(n)$ is independent and identically distributed sequence matrix.

2. $\tilde{\mathbf{h}}(n)$ is independent of $\mathbf{U}_i(n)$

Now, taking the expectation from both sides of (52) and using the fact that $\mathbf{e}_{i,D}(n) = \mathbf{U}_i^T(n)\tilde{\mathbf{h}}(n) + \mathbf{v}_{i,D}(n)$, the third term in the right-hand side of (52) is simplified by

$$\begin{aligned} \sum_{i=0}^{N-1} E\{\mathbf{v}_{i,D}^T(n)(\mathbf{U}_i^T(n)\mathbf{U}_i(n))^{-1}\mathbf{e}_{i,D}(n)\} = \\ \sum_{i=0}^{N-1} E\{\mathbf{v}_{i,D}^T(n)(\mathbf{U}_i^T(n)\mathbf{U}_i(n))^{-1}\mathbf{v}_{i,D}(n)\} = \\ \sum_{i=0}^{N-1} \sigma_{v_{i,D}}^2 \text{Tr}(E[\mathbf{U}_i^T(n)\mathbf{U}_i(n)]^{-1}), \end{aligned} \quad (53)$$

where $E\{\mathbf{v}_{i,D}(n)\mathbf{v}_{i,D}^T(n)\} = \sigma_{v_{i,D}}^2 \mathbf{I}$. Substituting (53) into (54), we obtain

$$\begin{aligned} E \|\tilde{\mathbf{h}}(n+1)\|^2 = E \|\tilde{\mathbf{h}}(n)\|^2 \\ - 2\mu \sum_{i=0}^{N-1} E[\mathbf{e}_{i,D}^T(n)(\mathbf{U}_i^T(n)\mathbf{U}_i(n))^{-1}\mathbf{e}_{i,D}(n)] \\ + 2\mu \sum_{i=0}^{N-1} \sigma_{v_{i,D}}^2 \text{Tr}(E[\mathbf{U}_i^T(n)\mathbf{U}_i(n)]^{-1}) \\ + 2\mu\kappa \sum_{i=0}^{N-1} E[\mathbf{f}^T(\mathbf{h}(n))\mathbf{U}_i(n)(\mathbf{U}_i^T(n)\mathbf{U}_i(n))^{-1}\mathbf{e}_{i,D}(n)] \\ + \mu^2 \sum_{i=0}^{N-1} E[\mathbf{e}_{i,D}^T(n)(\mathbf{U}_i^T(n)\mathbf{U}_i(n))^{-1}\mathbf{e}_{i,D}(n)] \\ - \kappa E[\mathbf{f}^T(\mathbf{h}(n))\tilde{\mathbf{h}}(n)] + \kappa^2 E[\|\mathbf{f}(\mathbf{h}(n))\|^2], \end{aligned} \quad (54)$$

To simplify the recent relation, we assume that matrix, $\mathbf{U}_i^T(n)\mathbf{U}_i(n)$, is diagonal. This assumption was successfully applied in [10] and [11]. Using this assumption leads to

$$\begin{aligned} E \|\tilde{\mathbf{h}}(n+1)\|^2 = E \|\tilde{\mathbf{h}}(n)\|^2 \\ - \mu(2-\mu) \sum_{i=0}^{N-1} E\left\{\left(\frac{e_{i,D}^2(n) - 2\sigma_{v_{i,D}}^2/(2-\mu)}{\|\mathbf{u}_i(n)\|^2}\right)\right. \\ \left. + \left(\frac{e_{i,D}^2(n-1) - 2\sigma_{v_{i,D}}^2/(2-\mu)}{\|\mathbf{u}_i(n-1)\|^2}\right) + \dots\right. \\ \left. + \left(\frac{e_{i,D}^2(n-K+1) - 2\sigma_{v_{i,D}}^2/(2-\mu)}{\|\mathbf{u}_i(n-K+1)\|^2}\right)\right\} \\ + 2\mu\kappa \sum_{i=0}^{N-1} E[\mathbf{f}^T(\mathbf{h}(n))\mathbf{U}_i(n)(\mathbf{U}_i^T(n)\mathbf{U}_i(n))^{-1}\mathbf{e}_{i,D}(n)] \\ - \kappa E[\mathbf{f}^T(\mathbf{h}(n))\tilde{\mathbf{h}}(n)] + \kappa^2 E[\|\mathbf{f}(\mathbf{h}(n))\|^2], \end{aligned} \quad (55)$$

The mean square deviation (MSD) and mean square error (MSE) are obtained by

$$MSD(n) = E \|\tilde{\mathbf{h}}(n)\|^2, \quad (56)$$

$$MSE(n) = E[e_{i,D}^2(n)], \quad (57)$$

Therefore,

$$\begin{aligned} MSD(n+1) = MSD(n) \\ - \mu(2-\mu) \sum_{i=0}^{N-1} \left(\frac{MSE(n) - 2\sigma_{v_{i,D}}^2/(2-\mu)}{E\|\mathbf{u}_i(n)\|^2}\right) \\ - \mu(2-\mu) \sum_{i=0}^{N-1} \left(\frac{MSE(n-1) - 2\sigma_{v_{i,D}}^2/(2-\mu)}{E\|\mathbf{u}_i(n-1)\|^2}\right) - \dots \\ - \mu(2-\mu) \sum_{i=0}^{N-1} \left(\frac{MSE(n-K+1) - 2\sigma_{v_{i,D}}^2/(2-\mu)}{E\|\mathbf{u}_i(n-K+1)\|^2}\right) \\ + 2\mu\kappa \sum_{i=0}^{N-1} E[\mathbf{f}^T(\mathbf{h}(n))\mathbf{U}_i(n)(\mathbf{U}_i^T(n)\mathbf{U}_i(n))^{-1}\mathbf{e}_{i,D}(n)] \\ - \kappa E[\mathbf{f}^T(\mathbf{h}(n))\tilde{\mathbf{h}}(n)] + \kappa^2 E[\|\mathbf{f}(\mathbf{h}(n))\|^2], \end{aligned} \quad (58)$$

The recent relation can be rearranged as

$$\begin{aligned} MSD(n+1) = MSD(n) \\ - \mu(2-\mu) \sum_{i=0}^{N-1} \left(\frac{MSE(n)}{E\|\mathbf{u}_i(n)\|^2} + \dots + \frac{MSE(n-K+1)}{E\|\mathbf{u}_i(n-K+1)\|^2}\right) \\ + 2\mu \sum_{i=0}^{N-1} \sigma_{v_{i,D}}^2 \left(\frac{1}{E\|\mathbf{u}_i(n)\|^2} + \dots + \frac{1}{E\|\mathbf{u}_i(n-K+1)\|^2}\right) \\ + 2\mu\kappa \sum_{i=0}^{N-1} E[\mathbf{f}^T(\mathbf{h}(n))\mathbf{U}_i(n)(\mathbf{U}_i^T(n)\mathbf{U}_i(n))^{-1}\mathbf{e}_{i,D}(n)] \\ - \kappa E[\mathbf{f}^T(\mathbf{h}(n))\tilde{\mathbf{h}}(n)] + \kappa^2 E[\|\mathbf{f}(\mathbf{h}(n))\|^2], \end{aligned} \quad (59)$$

when n goes to infinity, $MSD(n+1) = MSD(n)$, $MSE(n) = MSE(n-1) = \dots = MSE(n-K+1)$, and $E\|\mathbf{u}_i(n)\|^2 = M\sigma_{u_i}^2$. Therefore, the above relation becomes

$$\begin{aligned} \mu(2-\mu) \sum_{i=0}^{N-1} \left(\frac{MSE}{M\sigma_{u_i}^2} + \dots + \frac{MSE}{M\sigma_{u_i}^2}\right) = \\ \sum_{i=0}^{N-1} \left(\frac{1}{M\sigma_{u_i}^2} + \dots + \frac{1}{M\sigma_{u_i}^2}\right) \\ + 2\mu \sum_{i=0}^{N-1} \sigma_{v_{i,D}}^2 \left(\frac{1}{M\sigma_{u_i}^2} + \dots + \frac{1}{M\sigma_{u_i}^2}\right) \\ + 2\mu\kappa \sum_{i=0}^{N-1} E[\mathbf{f}^T(\mathbf{h}(n))\mathbf{U}_i(n)(\mathbf{U}_i^T(n)\mathbf{U}_i(n))^{-1}\mathbf{e}_{i,D}(n)] \\ - \kappa E[\mathbf{f}^T(\mathbf{h}(n))\tilde{\mathbf{h}}(n)] + \kappa^2 E[\|\mathbf{f}(\mathbf{h}(n))\|^2], \end{aligned} \quad (60)$$

Equation (60) can be simplified as

$$\begin{aligned} \frac{\mu(2-\mu)}{M} MSE \sum_{i=0}^{N-1} \frac{P}{\sigma_{u_i}^2} = \frac{2\mu}{M} \sum_{i=0}^{N-1} \frac{P\sigma_{v_{i,D}}^2}{\sigma_{u_i}^2} \\ + \{\text{term with } \mathbf{f}(\mathbf{h}(n))\} \end{aligned} \quad (61)$$

Finally, the steady-state MSE is given by

$$\begin{aligned} MSE = \frac{2 \sum_{i=0}^{N-1} \frac{P\sigma_{v_{i,D}}^2}{\sigma_{u_i}^2}}{(2-\mu) \sum_{i=0}^{N-1} \frac{1}{\sigma_{u_i}^2}} \\ + \frac{\{\text{term with } \mathbf{f}(\mathbf{h}(n))\}}{\frac{\mu(2-\mu)P}{M} \sum_{i=0}^{N-1} \frac{1}{\sigma_{u_i}^2}}, \end{aligned} \quad (62)$$

The first term in the right-hand side of (62) is the steady-state MSE of IMSAF. The second term is related to L_0 -IMSAF. Using $\kappa = \mu\delta$, we have

$$\begin{aligned} \frac{BS-IMSAF}{MSE} = \frac{IMSAF}{MSE} \\ + \frac{2\mu\delta \sum_{i=0}^{N-1} E[\mathbf{f}^T(\mathbf{h}(n))\mathbf{U}_i(n)(\mathbf{U}_i^T(n)\mathbf{U}_i(n))^{-1}\mathbf{e}_{i,D}(n)]}{\frac{(2-\mu)P}{M} \sum_{i=0}^{N-1} \frac{1}{\sigma_{u_i}^2}} \\ + \frac{-\delta E[\mathbf{f}^T(\mathbf{h}(n))\tilde{\mathbf{h}}(n)] + \mu\delta^2 E[\|\mathbf{f}(\mathbf{h}(n))\|^2]}{\frac{(2-\mu)P}{M} \sum_{i=0}^{N-1} \frac{1}{\sigma_{u_i}^2}} \end{aligned} \quad (63)$$

By defining $a = \mu E\|\mathbf{f}(\mathbf{h}(n))\|^2$ and

$$\begin{aligned} b \\ = 2\mu \sum_{i=0}^{N-1} E[\mathbf{f}^T(\mathbf{h}(n))\mathbf{U}_i(n)(\mathbf{U}_i^T(n)\mathbf{U}_i(n))^{-1}\mathbf{e}_{i,D}(n)] \\ - E[\mathbf{f}^T(\mathbf{h}(n))\tilde{\mathbf{h}}(n)], \end{aligned} \quad (64)$$

the MSE relation becomes

$$\overbrace{MSE}^{BS-IMSAF} = \overbrace{MSE}^{IMSAF} + \frac{\delta^2 a + \delta b}{\frac{(2-\mu)^P}{M} \sum_{i=0}^{N-1} \frac{1}{\sigma_{u_i}^2}}, \quad (65)$$

Since $0 < \mu < 2$, the denominator of second term in the right-hand side of (65) is positive, i.e. $\frac{(2-\mu)^P}{M} \sum_{i=0}^{N-1} \frac{1}{\sigma_{u_i}^2} > 0$. Therefore, if $\delta^2 a + \delta b < 0$, then the MSE of family of BS-IMSAF algorithms will be lower than IMSAF. In the following, we find the condition for δ when $\delta^2 a + \delta b < 0$. The condition is $\delta < -b/a$. Based on this, we obtain

$$\delta < \frac{-2\mu \sum_{i=0}^{N-1} E[\mathbf{f}^T(\mathbf{h}(n))\mathbb{U}_i(n)(\mathbb{U}_i^T(n)\mathbb{U}_i(n))^{-1}\mathbb{e}_{i,D}(n)]}{\mu E[\|\mathbf{f}(\mathbf{h}(n))\|^2]} + \frac{E[\mathbf{f}^T(\mathbf{h}(n))\tilde{\mathbf{h}}(n)]}{\mu E[\|\mathbf{f}(\mathbf{h}(n))\|^2]}. \quad (66)$$

By using $\mathbb{e}_{i,D}(n) = \mathbb{U}_i^T(n)\tilde{\mathbf{h}}(n) + v_{i,D}(n)$ and independence assumptions, we have

$$E[\mathbf{f}^T(\mathbf{h}(n))\mathbb{U}_i(n)(\mathbb{U}_i^T(n)\mathbb{U}_i(n))^{-1}\mathbb{e}_{i,D}(n)] \approx E[\mathbf{f}^T(\mathbf{h}(n))\tilde{\mathbf{h}}(n)]. \quad (67)$$

Based on (69), the following condition is achieved

$$\delta < \frac{-2\mu \sum_{i=0}^{N-1} E[\mathbf{f}^T(\mathbf{h}(n))\tilde{\mathbf{h}}(n)] + E[\mathbf{f}^T(\mathbf{h}(n))\tilde{\mathbf{h}}(n)]}{\mu E[\|\mathbf{f}(\mathbf{h}(n))\|^2]}, \quad (68)$$

Due to the analyze the relation in the steady-state, we need to replace the index n with ∞ in (68). By simplifying the recent relation, we obtain

$$\delta < \frac{(1 - 2\mu N)E[\mathbf{f}^T(\mathbf{h}(\infty))\tilde{\mathbf{h}}(\infty)]}{\mu E[\|\mathbf{f}(\mathbf{h}(\infty))\|^2]}, \quad (69)$$

Finally, the steady-state MSE in the family of BS-IMSAF algorithms is given by

$$\overbrace{MSE}^{BS-IMSAF} = \overbrace{MSE}^{IMSAF} + \frac{(2\mu N - 1)\delta E[\mathbf{f}^T(\mathbf{h}(\infty))\tilde{\mathbf{h}}(\infty)] + \mu\delta^2 E[\|\mathbf{f}(\mathbf{h}(\infty))\|^2]}{\frac{(2-\mu)^P}{M} \sum_{i=0}^{N-1} \frac{1}{\sigma_{u_i}^2}}, \quad (70)$$

Computational Complexity

Table 7 presents the computational complexity of the IMSAF and the proposed algorithms in terms of the number of multiplications per iteration for real data. In this table, M is the filter length, N is the number of subbands, K is the number of input regressors, Q is the length of channel filters, L is the length of blocks, S is the number of selected input regressors, and $S_i(k)$ is the number of selected regressors at each subband which is dynamic. This table indicates that the number of multiplications in BS-IMSAF depends on K . But, in BS-SR-IMSAF and BS-DSR-IMSAF, this parameter depends on S and $S_i(k)$. Therefore, the computational complexity of BS-SR-IMSAF and BS-DSR-IMSAF is lower than BS-IMSAF.

In the proposed algorithms, we have also additional $3M + LM$ multiplications and 1 division for the term of $\kappa\mathbf{f}(\mathbf{h}(n))$.

Table 7: The number of multiplications in IMSAF, BS-IMSAF, BS-SR-IMSAF, and BS-DSR-IMSAF algorithms

Algorithm	Number of Multiplications
IMSAF	$(K^2 + 2K)M + K^3 + K^2 + 3NQ$
BS-IMSAF [*]	$(K^2 + 2K + 3)M + K^3 + K^2 + 3NQ + LM$
BS-SR-IMSAF [*]	$(S^2 + 2S + 3)M + S^3 + S^2 + 2M(K - S) + 2K + 3NQ + LM$
BS-DSR-IMSAF [*]	$\sum_{i=0}^{N-1} \frac{1}{N} [(S_i^2(k) + S_i(k) + K)M + S_i^3(k) + S_i^2(k) + 3NQ + 3M + LM]$

* Proposed in this paper.

Simulation Results

The performance of the proposed algorithms is evaluated by computer simulations in the system identification. To generate block sparse of impulse response, the Markov-Gaussian model is used as

$$P\{s_k = 0 | s_{k-1} = 0\} = p_1,$$

$$P\{s_k \neq 0 | s_{k-1} \neq 0\} = p_2.$$

where $p_1 = 0.99$, and $p_2 = 0.91$ [27]. The nonzero coefficients are generated according to the white Gaussian noise. The input signal is an AR(1) signal which is generated by passing a zero-mean white Gaussian noise through a first-order system $H(z) = \frac{1}{1-0.9z^{-1}}$. An additive white Gaussian noise was added to the system output, which sets the signal-to-noise ratio (SNR) to 40 dB. In all simulations, we show the normalized mean square deviation (NMSD), $10\log_{10}(\frac{\|\mathbf{h}(n) - \mathbf{h}^0\|^2}{\|\mathbf{h}^0\|^2})$, which is evaluated by ensemble averaging over 200 independent trials. Table 8 shows the values of the parameters in the simulations. The impulse response of the unknown block sparse system with $M = 800$ has been presented in Fig. 3.

Fig. 4 shows the steady-state NMSD values versus κ for the family of BS-IMSAF algorithms. The values of κ changes from 10^{-8} to 10^{-3} . The optimum values for κ are observed in this simulation. Table 9 specifies the exact optimum values of κ . We observe that, the BS-NSAF and the family of BS-IMSAF algorithms have close optimum values. Fig. 5 shows the NMSD learning curves in optimum values of κ for conventional and block sparse adaptive algorithms. We compared the learning curves of the proposed algorithms with NSAF [7], IMSAF [9], and L_0 -NSAF [19] algorithms. The block sparse adaptive

algorithms show better convergence speed and lower steady-state error than classical NSAF and IMSAF algorithms. In comparison with BS adaptive algorithms, the NSAF and IMSAF algorithms have larger steady-state error. Also, the L_0 -NSAF has larger steady-state error than BS adaptive algorithms.

Table 8: The values of the parameters in the simulations ($M = 800, S = 2$, and $\sigma_v^2 = 10^{-4}$).

Figure	N	K	L	μ	κ
— Performance for changing κ :					
Fig. 4	8	2	2	1	$10^{-8}, \dots, 10^{-3}$
Fig. 5	8	2	2	1	$\{1.7, 3.8, 8.5\} \times 10^{-6}$
Fig. 56	4	8	2	0.5	$10^{-8}, \dots, 10^{-3}$
Fig. 7	4	8	2	0.5	$\{0.36, 1.74, 2.59\} \times 10^{-6}$
— Performance of Changing L :					
Fig. 8	4	8	1, ..., 50	0.5	1.74×10^{-6}
— Performance for changing K :					
Fig. 10	4	2, ..., 8	5	0.5	5.5×10^{-6}
Fig. 11	4	2, ..., 8	5	0.5	5.5×10^{-6}
Fig. 12	4	2, ..., 8	5	0.5	5.5×10^{-6}

Table 9: Optimum values of κ in Figs. 4 and 6.

Algorithm	Optimum values of κ in Fig. 4	Optimum values of κ in Fig. 6
L_0 -NSAF	1.7×10^{-6}	0.36×10^{-6}
BS-NSAF	8.5×10^{-6}	2.59×10^{-6}
BS-IMSAF	8.5×10^{-6}	2.59×10^{-6}
BS-SR-IMSAF	8.5×10^{-6}	2.59×10^{-6}
BS-DSR-IMSAF	3.8×10^{-6}	1.74×10^{-6}

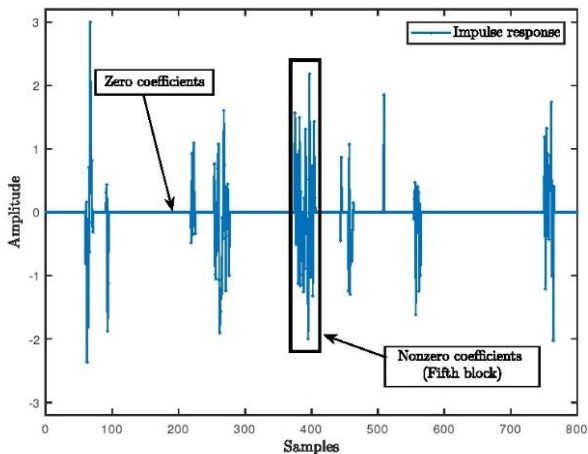


Fig. 3: The impulse response of unknown block sparse system.

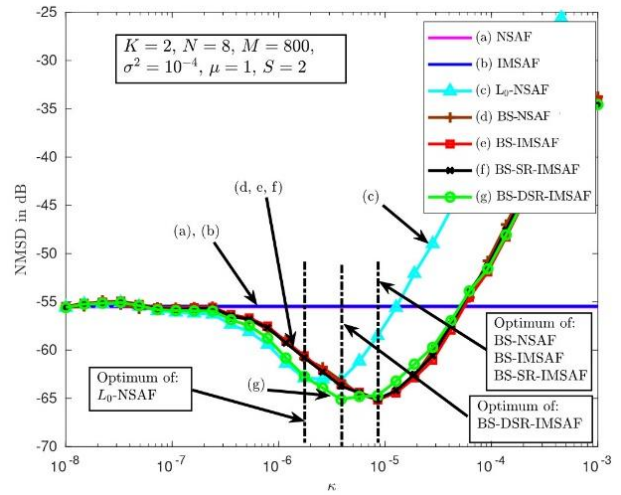


Fig. 4: The steady-state NMSD versus κ for the proposed algorithms ($M = 800, N = 8$, and $K = 2$).

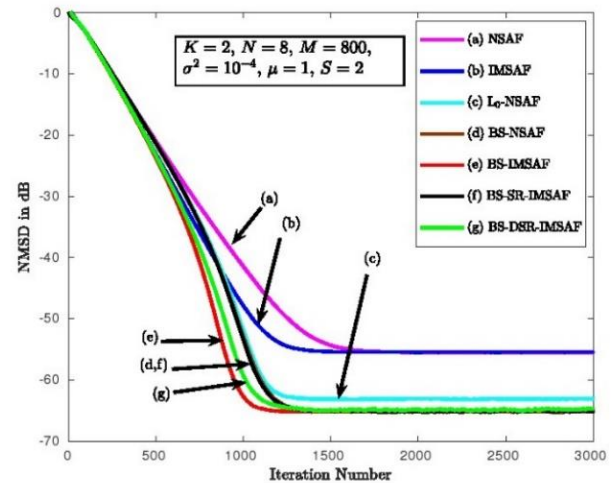


Fig. 5: The NMSD learning curves of all algorithms in the optimum values of κ ($M = 800, N = 8$, and $K = 2$).

Fig. 6 presents the steady-state NMSD values versus κ for the family of subband adaptive filter algorithms according to the parameters in Table 8.

Again, optimum values are obtained for block sparse adaptive filter algorithms. Table 9 shows the exact optimum values of κ in this simulation. We observe that BS-NSAF, BS-IMSAF, and BS-SR-NSAF have the same optimum values.

The BS-DSR-IMSAF has slightly lower optimum value than other BS algorithms. Fig. 7 compares the NMSD learning curves of classical and block sparse adaptive algorithms. This figure indicates that the proposed block sparse adaptive algorithms have better performance than NSAF, IMSAF, and L_0 -NSAF algorithms. The performance of BS-SR-IMSAF and BS-DSR-IMSAF are close to the BS-IMSAF.

Furthermore, the steady-state NMSD of BS-SR-IMSAF and BS-DSR-IMSAF algorithms are lower than BS-IMSAF.

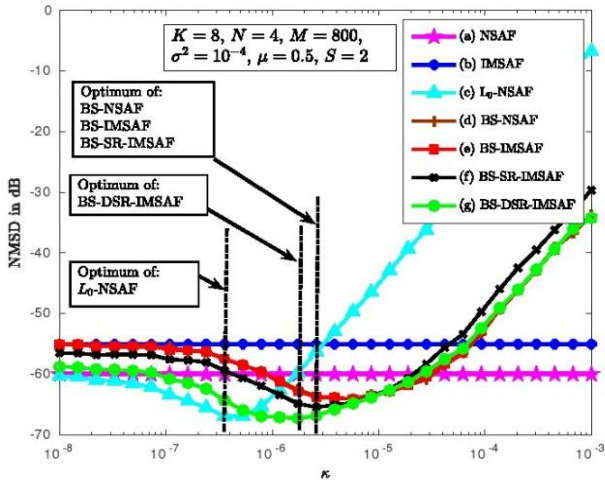


Fig. 6: The steady-state NMSD versus κ for the proposed algorithms ($M = 800$, $N = 4$, and $K = 8$).

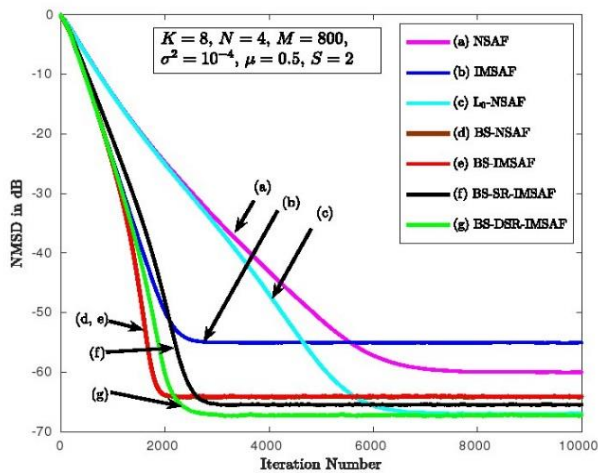


Fig. 7: The NMSD learning curves of all algorithms in the optimum values of κ ($M = 800$, $N = 4$, and $K = 8$).

In Fig. 8, we change the value of L and plot the steady-state NMSD values versus L . The values of L change from 1 to 50. The other parameters are set according to the Table 8. As we see, for $L=5$, the steady-state NMSD is obtained. Since the optimum value of κ changes between 10^{-5} and 10^{-6} , we select the midpoint value, 5.5×10^{-6} , for κ . Therefore, in the following simulations, we set the parameter L to 5 and the value of κ is set to 5.5×10^{-6} . Fig. 9 shows the performance of BS-IMSAF for different values of K . By increasing K , the convergence speed increases. But, the steady-state error also increases. The performance of BS-IMSAF is significantly better than other algorithms. Fig. 10 compares the learning curves of BS-SR-IMSAF and BS-IMSAF algorithm. We see that the BS-SR-IMSAF has the same performance as BS-IMSAF. But, the computational complexity of BS-SR-IMSAF is lower than BS-IMSAF. Fig. 11 investigates the performance of BS-DSR-IMSAF algorithm. Good performance can be seen for BS-DSR-IMSAF. By increasing the parameter K , the convergence speed of BS-DSR-

IMSAF is faster than BS-IMSAF. Also, for BS-DSR-IMSAF, the same steady-state NMSD as BS-IMSAF is observed.

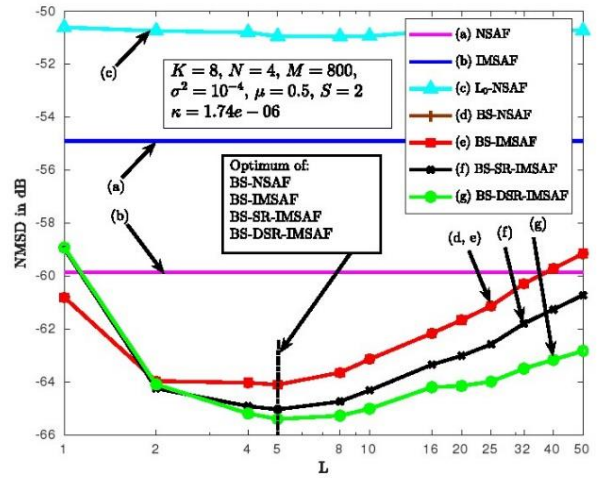


Fig. 8: The steady-state NMSD versus L , length of block, for NSAF, IMSAF and proposed BS-IMSAF algorithms ($M = 800$, $N = 4$, and $K = 8$).

Fig. 12 shows the number of selected regressors at each subband during the adaptation. This figure indicates that in the steady-state, the number of selected regressors converged to 1. It means that the steady-state error of this algorithm becomes low even for large values of K . Table 10 shows the simulated and theoretical steady-state NMSD for different values of SNR. These values are obtained for BS-IMSAF, BS-SR-IMSAF, and BS-DSR-IMSAF algorithms. As we see, the good agreement between simulated and theoretical steady-state NMSD values is observed. Table 11 compares the computation time and the values of NMSD in different algorithms at iterations 2000 and 3000. The parameters of the algorithms are according to the Fig. 9. This table indicates that the NMSD values of BS adaptive algorithms at iterations 2000 and 3000 are significantly lower than NSAF, IMSAF and L_0 -NSAF algorithms.

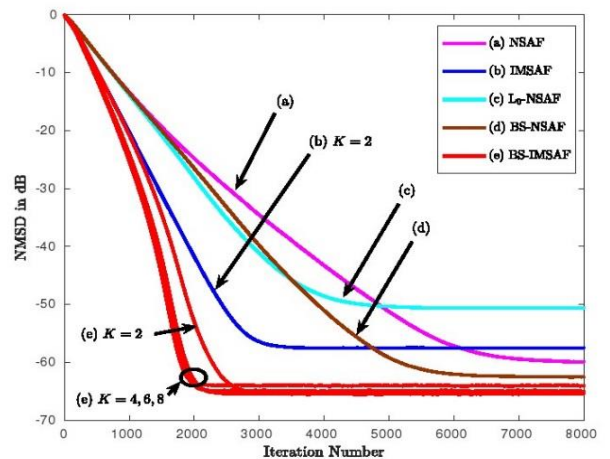


Fig. 9: The simulated and theoretical steady-state NMSD for different values of SNR ($M = 800$, $N = 4$, $K = 8$, $\mu = 0.5$).

Table 10: The simulated and theoretical steady-state NMSD for different values of SNR ($M = 800, N = 4, K = 8, \mu = 0.5$)

Algorithm	BS-IMSAF	BS-SR-IMSAF	BS-DSR-IMSAF
Simulation (SNR=10dB)	-14.45	-14.72	-14.85
Theory (SNR=10dB)	-15.21	-15.81	-15.90
Simulation (SNR=20dB)	-29.50	-29.60	-29.62
Theory (SNR=20dB)	-30.40	-30.35	-30.51
Simulation (SNR=40dB)	-64.81	-64.85	-64.89
Theory (SNR=40dB)	-65.20	-65.12	-65.20

Table 11: The computation time and the values of the NMSD in different algorithms at iterations 2000 and 3000

Algorithm	Time (s)		NMSD in dB	
	2000	3000	2000	3000
NSAF	2.2	3.3	-23.9	-34.5
IMSAF	56.4	84.6	-39.2	-57.2
L_0 -NSAF	2.9	4.3	-26.3	-41.1
BS-NSAF	4.5	6.4	-25.1	-40.5
BS-IMSAF	56.9	85.5	-54.2	-64.8
BS-SR-IMSAF	14.5	21.7	-54.2	-64.8
BS-DSR-IMSAF	26.6	40.5	-63.5	-64.8

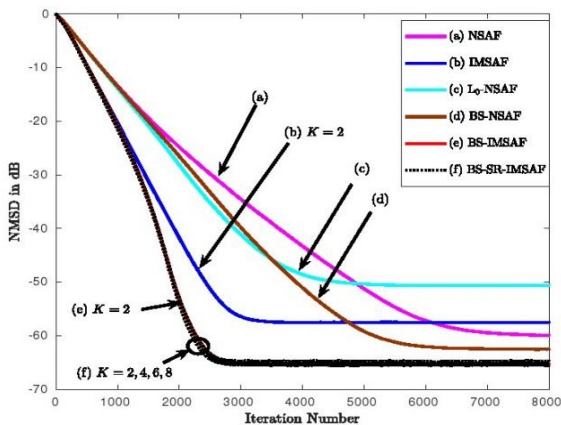


Fig. 10: The NMSD learning curves for different values of K , number of recent regressors in BS-SR-IMSAF algorithm ($\kappa = 5.5 \times 10^{-6}, M = 800, N = 4, K = 2, 4, 6, 8$).

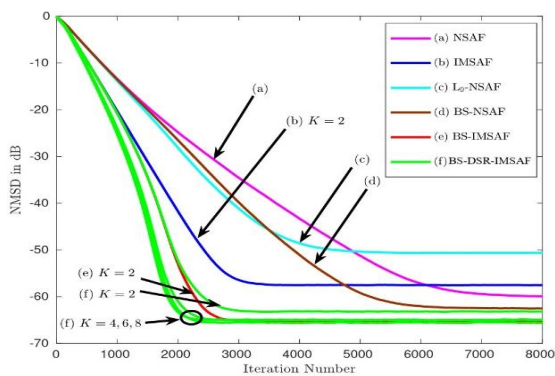


Fig. 11: The NMSD learning curves for different values of K , number of recent regressors in BS-DSR-IMSAF algorithm ($\kappa = 5.5 \times 10^{-6}, M = 800, N = 4, K = 2, 4, 6, 8$).

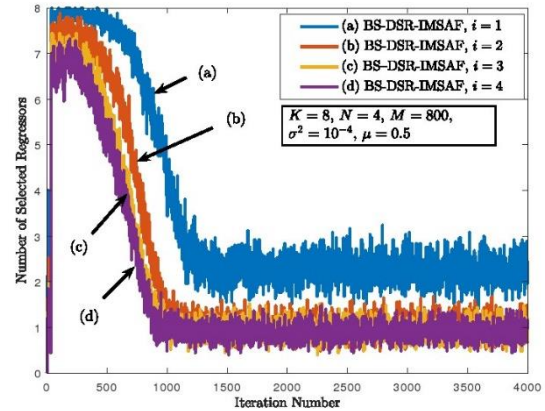


Fig. 12: The number of selected regressors at each subband in BS-DSR-IMSAF algorithm ($M = 800, N = 4$, and $K = 8$).

Summary and Conclusion

This paper presented the family of IMSAF algorithms for block sparse system identification. In the first algorithm, the BS-NSAF was introduced. This algorithm had better performance than NSAF for BS system identification. In the following the BS-IMSAF was presented. The proposed algorithm had better convergence speed than BS-NSAF. To reduce the computational complexity, the BS-SR-IMSAF and BS-DSR-IMSAF algorithms were developed. These algorithms had close performance to BS-IMSAF. Furthermore, the theoretical steady-state behavior of the proposed algorithms was studied.

Author Contributions

All authors contributed to all part of preparing and writing of this paper.

Acknowledgment

The authors would like to thank the editor and anonymous reviewers.

Conflict of Interest

The authors declare no potential conflict of interest regarding the publication of this work. In addition, the ethical issues including plagiarism, informed consent, misconduct, data fabrication and, or falsification, double publication and, or submission, and redundancy have been completely witnessed by the authors.

Abbreviations

LMS	Least Mean Squares
APA	Affine Projection Algorithm
NSAF	Normalized Subband Adaptive Filter
IMSAF	Improved Multiband Structured Subband Adaptive Filter
BS	Block Sparse
MSE	Mean Square Error
NMSD	Normalized Mean Square Deviation

References

- [1] B. Widrow, S. D. Stearns, *Adaptive Signal Processing*, Englewood Cliffs, NJ: Prentice-Hall, 1985.
- [2] J. R. Treichler, C. R. Johnson, M. G. Larimore, *Theory and Design of Adaptive Filters*, Wiley, 1987.
- [3] S. Haykin, *Adaptive Filter Theory*, NJ: Prentice-Hall, 4th edition, 2002.
- [4] A. H. Sayed, *Adaptive Filters*, Wiley, 2008.
- [5] B. Farhang-Boroujeny, *Adaptive Filters: Theory and Applications*, Wiley, 1998.
- [6] K. Ozeki, T. Umeda, "An adaptive filtering algorithm using an orthogonal projection to an affine subspace and its properties, *Electron. Commun. Jpn.*, 67-A: 19–27, 1984.
- [7] K. A. Lee, W. S. Gan, "Improving convergence of the NLMS algorithm using constrained subband updates," *IEEE Signal Process. Lett.*, 11 (9): 736–739, 2004.
- [8] F. Yang, M. Wu, P. Ji, J. Yang, "An improved multiband-structured subband adaptive filter algorithm," *IEEE Signal Process. Lett.*, 19: 647–650, 2012.
- [9] F. Yang, M. Wu, P. Ji, J. Yang, "Low-complexity implementation of the improved multiband-structured subband adaptive filter algorithm," *IEEE Trans. Signal Process.*, 63: 5133–5148, 2015.
- [10] K. Y. Hwang, W. J. Song, "An affine projection adaptive filtering algorithm with selective regressors," *IEEE Trans. Circuits Syst. II Express Briefs*, 54(1): 43–46, 2007.
- [11] S. J. Kong, K. Y. Hwang, W. J. Song, "An affine projection algorithm with dynamic selection of input vectors," *IEEE Signal Process. Lett.*, 14(8): 529–532, 2007.
- [12] M. S. E. Abadi, J. H. Husoy, M. J. Ahmadi, "Two improved multiband structured subband adaptive filter algorithms with reduced computational complexity," *Signal Process.*, 154: 15–29, 2019.
- [13] M. S. E. Abadi, M. J. Ahmadi, "Weighted improved multiband-structured subband adaptive filter algorithms," *IEEE Trans. Circuits Syst. II Express Briefs*, 2019.
- [14] M. S. E. Abadi, M. J. Ahmadi, "Diffusion improved multiband-structured subband adaptive filter algorithm with dynamic selection of nodes over distributed networks," *IEEE Trans. Circuits Syst. II Express Briefs*, 66(3): 507–511, 2018.
- [15] M. S. E. Abadi, H. Mesgarani, S. M. Khademiyan, "The wavelet transform-domain LMS adaptive filter employing dynamic selection of subband-coefficients," *Digital Signal Process.*, 69: 94–105, 2017.
- [16] D. L. Duttweiler, "Proportionate normalized least-mean-squares adaptation in echo cancellers," *IEEE Trans. Speech Audio Process.*, 8(5): 508–518, 2000.
- [17] A. Steingass, A. Lehner, F. Perez-Fontan, E. Kubista, B. Arbesser-Rastburg, "Characterization of the aeronautical satellite navigation channel through high-resolution measurement and physical optics simulation," *Int. J. Satell. Commun. Netw.*, 269: 1–305, 2008.
- [18] Y. Gu, J. Jin, S. Mei, " l_0 norm constraint LMS algorithm for sparse system identification," *IEEE Signal Process. Lett.*, 16(9): 774–777, 2009.
- [19] Y. Yu, H. Zhao, B. Chen, "Sparse normalized subband adaptive filter algorithm with l_0 -norm constraint," *J. Franklin Inst.*, 353(18): 5121–5136, 2016.
- [20] M. Lima, W. Martins, P. S. R. Diniz, "Affine projection algorithms for sparse system identification," in *Proc. ICASSP*: 5666–5670, 2013.
- [21] M. Lima, T. Ferreira, W. Martins, P. S. R. Diniz, "Sparsity-aware data-selective adaptive filters," *IEEE Trans. Signal Process.*, 62 (17): 4557–4572, 2014.
- [22] L. Ji, J. NiK., "Sparsity-aware normalized subband adaptive filters with jointly optimized parameters," *J. Franklin Inst.*, 357(17): 13144–13157, 2020.
- [23] Y. Yu, T. Yang, H. Chen, R. Lamare, Y. Li, "Sparsity-aware SSAF algorithm with individual weighting factors: Performance analysis and improvements in acoustic echo cancellation," *Signal Process.*, 178(1): 1–16, 2021.
- [24] Y. Yu, H. Zhao, R. Lamare, L. Lu, "Sparsity-aware subband adaptive algorithms with adjustable penalties," *Digital Signal Process.*, 84(1): 93–106, 2019.
- [25] Z. Habibi, H. Zayyani, M. S. E. Abadi, "A robust subband adaptive filter algorithm for sparse and block-sparse systems identification," *J. Syst. Eng. Electron.*, 32(2): 487–497, 2021.
- [26] E. Heydari, M. S. E. Abadi, S. M. Khademiyan, "Improved multiband structured subband adaptive filter algorithm with l_0 -norm regularization for sparse system identification," *Digital Signal Process.*, 122(4): 1–14, 2022.
- [27] S. Jiang, Y. Gu, "Block-sparsity-induced adaptive filter for multi-clustering system identification," *IEEE Trans. Signal Process.*, 63(20): 5318–5330, 2015.
- [28] J. Liu, S. L. Grant, "Proportionate adaptive filtering for block-sparse system identification," *IEEE/ACM Trans. Audio Speech Lang. Process.*, 24(4): 623–629, 2016.
- [29] Z. Zhang, H. Zhao, "Affine projection M-estimate subband adaptive filters for robust adaptive filtering in impulsive noise," *Signal Process.*, 120 (3): 64–70, 2016.
- [30] H. C. Shin, A. H. Sayed, "Mean-Square performance of a family of affine projection algorithms," *IEEE Trans. Signal Process.*, 52(1): 90–102, 2004.

Biographies



Esmail Heydari received the B.S. degree in Electrical Engineering from Hakim Sabzevari University in 2011, and the M.S. degree in Electrical Engineering from Shahid Rajaei Teacher Training University, Tehran, Iran, in 2017. Currently, he is a Ph.D. candidate at the Faculty of Electrical Engineering, Shahid Rajaei Teacher Training University, Tehran, Iran. His research interests are adaptive filters and

adaptive distributed networks.

- Email: ehydari@sru.ac.ir
- ORCID: [0009-0005-4223-4176](https://orcid.org/0009-0005-4223-4176)
- Web of Science Researcher ID: NA
- Scopus Author ID: NA
- Homepage: NA



Mohammad Shams Esfand Abadi received the B.S. degree in Electrical Engineering from Mazandaran University, Mazandaran, Iran and the M.Sc. degree in Electrical Engineering from Tarbiat Modares University, Tehran, Iran in 2000 and 2002, respectively, and the Ph.D. degree in Biomedical Engineering from Tarbiat Modares University, Tehran, Iran in 2007. Since 2004 he has been with the Department of Electrical Engineering, Shahid Rajaei Teacher Training University, Tehran, Iran, where he is currently a

professor. His research interests include digital filter theory, adaptive distributed networks, and adaptive signal processing algorithms.

- Email: mshams@sru.ac.ir
- ORCID: [0000-0002-9856-6592](https://orcid.org/0000-0002-9856-6592)
- Web of Science Researcher ID: Y-7686-2019
- Scopus Author ID: 7006167272
- Homepage: <https://www.sru.ac.ir/shams/>



Seyed Mahmoud Khademiyan received the M.Sc. degree in Applied Mathematics from Iran University of Science and Technology, Tehran, Iran, in 2012. Currently, he is a Ph.D. candidate at the Department of Mathematics, Faculty of Science, Shahid Rajaei Teacher Training University, Tehran, Iran. His research interests include digital filter theory and adaptive signal processing algorithms.

- Email: m_khademiyan@sru.ac.ir
- ORCID: [0000-0002-9810-2819](https://orcid.org/0000-0002-9810-2819)
- Web of Science Researcher ID: NA
- Scopus Author ID: NA
- Homepage: NA

How to cite this paper:

E. Heydari, M. Shams Esfand Abadi, S. M. Khademiyan, "The new family of adaptive filter algorithms for block-sparse system identification," *J. Electr. Comput. Eng. Innovations*, 12(1): 133-146, 2024.

DOI: [10.22061/jecei.2023.10062.675](https://doi.org/10.22061/jecei.2023.10062.675)

URL: https://jecei.sru.ac.ir/article_1988.html

